



Sleep-stage-dependent alterations in cerebral oxygen metabolism quantified by magnetic resonance

Jing Xu¹ | Andrew Wiemken² | Michael C. Langham¹ | Hengyi Rao³ |
Marianne Nabbout¹ | Alessandra S. Caporale^{1,4,5}  | Richard J. Schwab² |
John A. Detre³ | Felix W. Wehrli¹ 

¹Laboratory for Structural, Physiological, and Functional Imaging, Department of Radiology, Perelman School of Medicine, University of Pennsylvania, Philadelphia, Pennsylvania, USA

²Division of Sleep Medicine, Department of Medicine, Perelman School of Medicine, University of Pennsylvania, Philadelphia, Pennsylvania, USA

³Department of Neurology, Perelman School of Medicine, University of Pennsylvania, Philadelphia, Pennsylvania, USA

⁴Department of Neurosciences, Imaging and Clinical Sciences, 'G. d'Annunzio University' of Chieti-Pescara, Chieti, Italy

⁵Institute for Advanced Biomedical Technologies (ITAB), 'G. d'Annunzio University' of Chieti-Pescara, Chieti, Italy

Correspondence

Felix W. Wehrli, Laboratory for Structural, Physiologic and Functional Imaging, University of Pennsylvania Perelman School of Medicine, Department of Radiology, 1 Founders Pavilion, 3400 Spruce Street, Philadelphia, PA 19104, USA.
Email: felix.wehrli@penncmedicine.upenn.edu

Present address

Jing Xu, Key Laboratory of Brain-Machine Intelligence for Information Behavior, Shanghai International Studies University, Shanghai, China.

Funding information

National Institutes of Health; National Institute of Biomedical Imaging and Bioengineering; National Institute of Aging; National Center for Advancing Translational Sciences, Grant/Award Number: UL1TR001878; National Institutes of Health (NIH), Grant/Award Number: R21 AG065816 and P41 EB029460

Abstract

A key function of sleep is to provide a regular period of reduced brain metabolism, which is critical for maintenance of healthy brain function. The purpose of this work was to quantify the sleep-stage-dependent changes in brain energetics in terms of cerebral metabolic rate of oxygen (CMRO₂) as a function of sleep stage using quantitative magnetic resonance imaging (MRI) with concurrent electroencephalography (EEG) during sleep in the scanner. Twenty-two young and older subjects with regular sleep hygiene and Pittsburgh Sleep Quality Index (PSQI) in the normal range were recruited for the study. Cerebral blood flow (CBF) and venous oxygen saturation (SvO₂) were obtained simultaneously at 3 Tesla field strength and 2.7-s temporal resolution during an 80-min time series using OxFlow, an in-house developed imaging sequence. The method yields whole-brain CMRO₂ in absolute physiologic units via Fick's Principle. Nineteen subjects yielded evaluable data free of subject motion artifacts. Among these subjects, 10 achieved slow-wave (N3) sleep, 16 achieved N2 sleep, and 19 achieved N1 sleep while undergoing the MRI protocol during scanning. Mean CMRO₂ was 98 ± 7 (μmol min⁻¹)/100g awake, declining progressively toward deepest sleep stage: 94 ± 10.8 (N1), 91 ± 11.4 (N2), and 76 ± 9.0 μmol min⁻¹/100g (N3), with each level differing significantly from the wake state. The technology described is able to quantify cerebral oxygen metabolism in absolute physiologic units along with non-REM sleep stage, indicating brain oxygen consumption to be closely associated with depth of sleep, with deeper sleep stages exhibiting progressively lower CMRO₂ levels.

KEYWORDS

cerebral blood flow, global cerebral metabolic rate of oxygen, non-REM sleep, venous oxygen saturation

1 | INTRODUCTION

Cerebral blood flow (CBF), venous and arterial oxygen saturation (SvO₂ and SaO₂), and cerebral metabolic rate of oxygen (CMRO₂) are key physiological parameters of brain function. Fick's Principle relates CMRO₂ to cerebral blood flow and the arterio-venous difference in O₂ saturation:

$$\text{CMRO}_2 = C_a \cdot \text{CBF} \cdot (\text{SaO}_2 - \text{SvO}_2) \quad (1)$$

with C_a being the oxygen carrying capacity of blood per unit volume, which is a function of hematocrit, and CBF expressed in units of volumetric blood flow per unit time and tissue mass (mlmin⁻¹/100g tissue). SaO₂ and SvO₂ are the percent oxygen saturation levels of arterial and venous blood, respectively. Cerebral hypometabolism has been observed in various prevalent neurological disorders, including Alzheimer's disease in studies carried out with ¹⁵O positron emission tomography (Mintun et al., 1984) have shown (Fukuyama et al., 1994; Ishii et al., 1996).

The healthy human brain is known to be highly active at all times, and increased neuronal activity necessitates a higher demand for oxygen and glucose extracted from arterial blood. In response to this increased demand, CBF tends to increase while SvO₂ decreases (Girouard & Iadecola, 2006). Thus, as neuronal activity increases, the brain undergoes physiological adjustments to ensure adequate supply of oxygen and nutrients to meet its metabolic needs (see, for instance, (Magistretti & Allaman, 2015)). Conversely, during lower metabolic states, including sleep (Boyle et al., 1994) and anesthesia (Oshima et al., 2002), CMRO₂ is adjusted downward. Whereas increases in CMRO₂ during functional activation are regional (see, for instance, [Fernandez-Seara et al., 2016; Kastrop et al., 2002]), reductions during sleep resulting from synaptic downscaling, affect the entire brain (Caporale et al., 2021; Madsen et al., 1991).

Sleep provides a regular period of reduced brain metabolism, which is critical for maintenance of healthy brain function. Fractured sleep, for example, or chronic partial sleep deprivation, may therefore result in oxidative injury due to the sustained high metabolic rate of the awake brain (Gopalakrishnan et al., 2004) and could be causative in the development of impaired cognition and executive function in older individuals. Further, sleep deprivation is known to cause reductions in antioxidants such as glutathione in the brain (D'Almeida et al., 1998).

The human sleep cycle consists of three non-rapid eye movement (Non-REM) sleep stages of increasing sleep depth defined as N1, N2, and N3 (also known as slow-wave or deep sleep) and rapid eye movement (REM) sleep (Al-Salman et al., 2023; Iber et al., 2007). Each sleep stage serves crucial functions in promoting mental and physical health and is essential for overall well-being.

Madsen et al., by means of the Kety-Schmidt technique, using ¹³³Xe as a tracer for quantifying CBF and blood gas analysis for assessing blood oxygen saturation, found that during deep sleep, CMRO₂ decreased by approximately 25% compared to wakefulness

Significance

The energy expenditures during sleep are reduced but the dependence of the cerebral metabolic rate of oxygen consumption (CMRO₂) during various sleep stages has not been known. Quantitative magnetic resonance imaging yielding neurometabolic parameter during sleep in the MRI scanner obtained with concurrent electroencephalographic mapping shows CMRO₂ to decrease during non-REM sleep relative to wakefulness, with the declines becoming progressively greater toward deeper sleep stages. The study thus provides new insights into the brain energetics during sleep.

(Madsen et al., 1991). Using similar methods, Boyle et al. (1994) found that during sleep both brain glucose utilization and oxygen metabolism fell by 17%. However, the techniques used in these studies are invasive, involving repeated simultaneous sampling of arterial and venous blood from the arterial and venous circulation and are thus not practical.

MRI is uniquely able to noninvasively quantify whole-brain CMRO₂ by combining measurements of CBF and SvO₂ (see, for instance, [Wehrli et al., 2017]). A method, referred to as OxFlow (as it simultaneously quantifies both parameters, oxygen saturation and flow) has been widely used to quantify CMRO₂ (Cao et al., 2018; Jain et al., 2010; Rodgers et al., 2013). In its original embodiment, the technique incorporates, in a single scan, measurement of blood flow rate in internal carotid and vertebral artery and SvO₂ from the phase of the blood water signal in the superior sagittal sinus (Jain et al., 2010). The latter is based on the method described in Fernández-Seara et al. (2006).

A recent study utilizing OxFlow with simultaneous EEG provided insights into the relationship between brain activity and CMRO₂ during EEG-verified slow-wave sleep (SWS) (Caporale et al., 2021). These studies have reported strong negative correlations between δ -power spectral density and CMRO₂. The observed decrements in CMRO₂ during SWS relative to wakefulness have ranged from 14% to 32%, indicating a reduction in cerebral metabolic activity during deep sleep. However, despite the progress made in understanding brain metabolism during deep sleep, the specific changes in brain metabolism during different sleep stages have not previously been explored.

In this study, we quantified CMRO₂ in 22 healthy subjects with OxFlow MRI and concurrent EEG recording for sleep staging. The OxFlow MRI technique enables the measurement of CMRO₂ with a temporal resolution of 2–3s during which CBF and SvO₂ are quantified. By evaluating CMRO₂ and examining its changes across different sleep stages, the present study provides new insights into the relationship between cerebral metabolism and sleep and thereby contributes to the understanding of the neural mechanisms underlying sleep and consciousness regulation.

2 | METHODS

2.1 | Participants and imaging protocol

The study protocol, illustrated in [Figure 1](#), was approved by the Institutional Review Board of the University of Pennsylvania (IRB# 832748). Fourteen young (six males, average age: 29 ± 4 years) and eight older healthy subjects (three males, average age: 67 ± 6 years) with regular sleep habits and BMI in the 18.5–30 range were recruited to participate in this study. All subjects had a Pittsburgh Sleep Quality Index (PSQI) (Buysse et al., 1989) in the normal range. Informed written consent was obtained from each subject. The imaging sessions were scheduled to take place between 09:00 p.m. and 12:00 a.m., aligning with the participants' typical circadian bedtime and occurrence of the initial sleep cycle.

2.2 | MRI data acquisition, processing, and analysis

MRI was performed on a 3T scanner (Siemens Prisma, Erlangen, Germany) using a 64-channel head–neck coil. The radial OxFlow sequence was used to quantify blood flow and SvO₂ in SSS (Cao et al., 2018). The MRI pulse sequence allowing time-course studies involving continuous scanning is illustrated in [Figure 2](#). The sequence yields blood flow velocity in the superior sagittal sinus (SSS) and, along with cross-sectional vessel area, cortical blood flow rate. In addition, from the phase of the signal, the relative magnetic susceptibility of venous blood is obtained, from which SvO₂ is computed (Jain et al., 2010). Scan parameters for the sequence were as follows: FOV = 240×240 mm², slice thickness = 5 mm, flip angle = 20°, TR = 40 ms, inter-echo spacing = 5 ms, velocity encoding (VENC) = 76.4 cm/s, first echo time (TE1) = 6.03 ms, duration = 80 min. Total CBF was obtained by upscaling the superior sagittal sinus blood flow, based on the blood flow-ratio obtained from a calibration scan (Rodgers et al., 2013). In this

manner, total brain CBF during the time series can be obtained from measurements of CBF in the superior sagittal sinus (that accounts for flow in the cerebral cortex only) and total flow obtained from internal carotid and vertebral arteries prior to the start of the sleep scan. The calibration scan parameters were as follows: FOV = 208×208 mm², slice thickness = 5 mm, flip angle = 15°, TR = 12 ms, velocity encoding (VENC) = 50 cm/s. T₁-weighted anatomic images were also acquired with MPRAGE to obtain brain tissue mass to normalize CMRO₂ (Jain et al., 2010). The parameters of MPRAGE were as follows: FOV = 224×224 mm², echo time = 2.43 ms, flip angle = 8°, inversion time = 900 ms, number of slices = 160, TR = 2200 ms.

Raw data from OxFlow k-space data were reconstructed with custom-designed MATLAB scripts (The MathWorks, Inc., Natick, MA, USA). The OxFlow sequence uses golden angle radial k-space sampling described previously (Cao et al., 2018), yielding an effective temporal resolution of 2.72 s ($2 \times TR \times 34$, with 2 the number of flow encodings and 34 the number of views in the central portion of k-space) corresponding to a total temporal footprint of 48.6 s. Velocity was computed from the phase difference of images reconstructed from the first echo acquired with two different settings of the gradient first moments. CBF at the SSS was calculated by averaging velocity over the ROI chosen that fully contains the SSS. Total CBF (tCBF) was quantified based on the BF-ratio obtained from the calibration scan (Caporale et al., 2023). Field maps were used to quantify SvO₂ in the SSS (Cao et al., 2018). The contribution of the static field inhomogeneity on tissue phase was corrected by fitting the background brain tissue surrounding the SSS to a second-order polynomial (Langham et al., 2009). The difference between the inter-echo phase accumulation of blood and background tissue was used to compute SvO₂ (Langham et al., 2009). Finally, CMRO₂ was computed via [Equation \(1\)](#) assuming SaO₂ of 98% since in healthy subjects during normal breathing arterial blood is fully saturated independent of state as shown previously (Caporale et al., 2021, 2023).

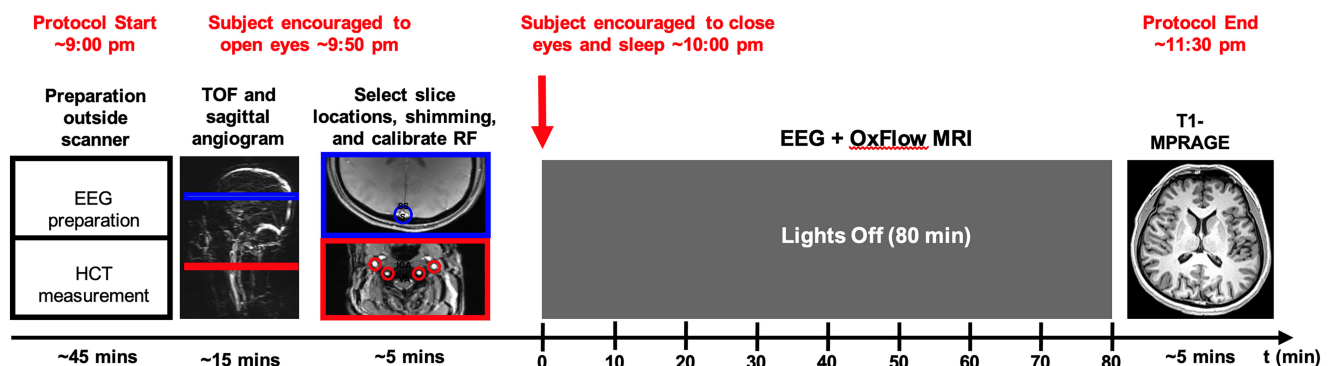


FIGURE 1 Illustration of study protocol. Following EEG set-up and measurement of hematocrit, sagittal MRI angiograms and axial scout images are acquired to prescribe neck and head imaging slices, and data are taken at the base of the skull and superior sagittal slices for quantification blood flow and venous oxygen saturation via OxFlow MRI (see [Figure 2](#)). The OxFlow sequence then is run at a temporal resolution of 2.72 s for a duration of 80 min while concurrent EEG recordings are obtained. Additionally, an anatomical image data set obtained with 3D MP-RAGE for determination of brain tissue mass, which is used for normalizing CMRO₂.

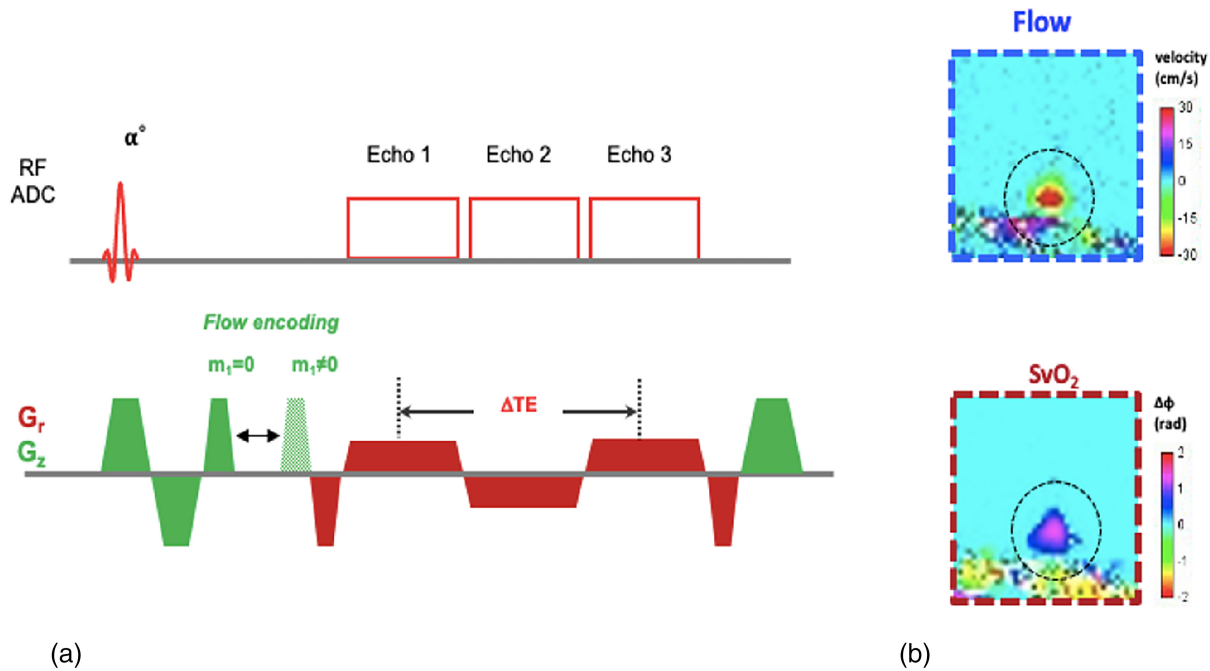


FIGURE 2 (a) Imaging pulse sequence collecting two echoes from which CBF and SvO₂ are obtained from measurements in the superior sagittal sinus (SSS). The phase difference from echoes 1 and 3 yields venous oxygen saturation whereas the phase difference obtained from echo 1, recorded with two settings of the flow-encoding gradient, yields blood flow velocity. (b) parametric images showing magnified cross-sectional views of the SSS for blood flow velocity and SvO₂.

2.3 | EEG data acquisition, processing, and analysis

EEG data were acquired using a 15-channel MR-compatible EEG system at a sampling rate of 5000 Hz (Brain Products, Gilching, Germany). EEG data processing was performed using BrainVision Analyzer software (Version 2.1, Brain Products, Gilching, Germany). First, MR gradient artifacts were removed using a sliding average of 31 segments (Allen et al., 2000), followed by down-sampling of the EEG data to 500 Hz. Pulse artifacts were removed by subtracting an average ECG artifact template. Independent component analysis (ICA) was used to further remove residual noise from the data. Finally, the EEG data underwent .5–30 Hz band-pass filtering and further down-sampling to 250 Hz.

Sleep stage was scored for every 30-s frame of preprocessed EEG data according to the American Academy of Sleep Medicine (AASM) criteria (Iber et al., 2007). Five discrete sleep stages were identified and scored: wakefulness (W), non-rapid eye movement (REM) stage 1 (N1), non-REM stage 2 (N2), non-REM stage 3 (N3), also referred to as slow-wave sleep (SWS) or deep sleep, and REM stage.

2.4 | Statistical analysis

CBF, SvO₂, and CMRO₂ were averaged over total duration of wakefulness and each non-REM sleep stage. One-way Repeated Measures ANOVA was used to compare the differences in these parameters during different sleep stages, post hoc test using

the Bonferroni correction was then applied to evaluate the significance of sleep-induced changes in the vascular-metabolic parameters.

3 | RESULTS

3.1 | Demographics and sleep statistics

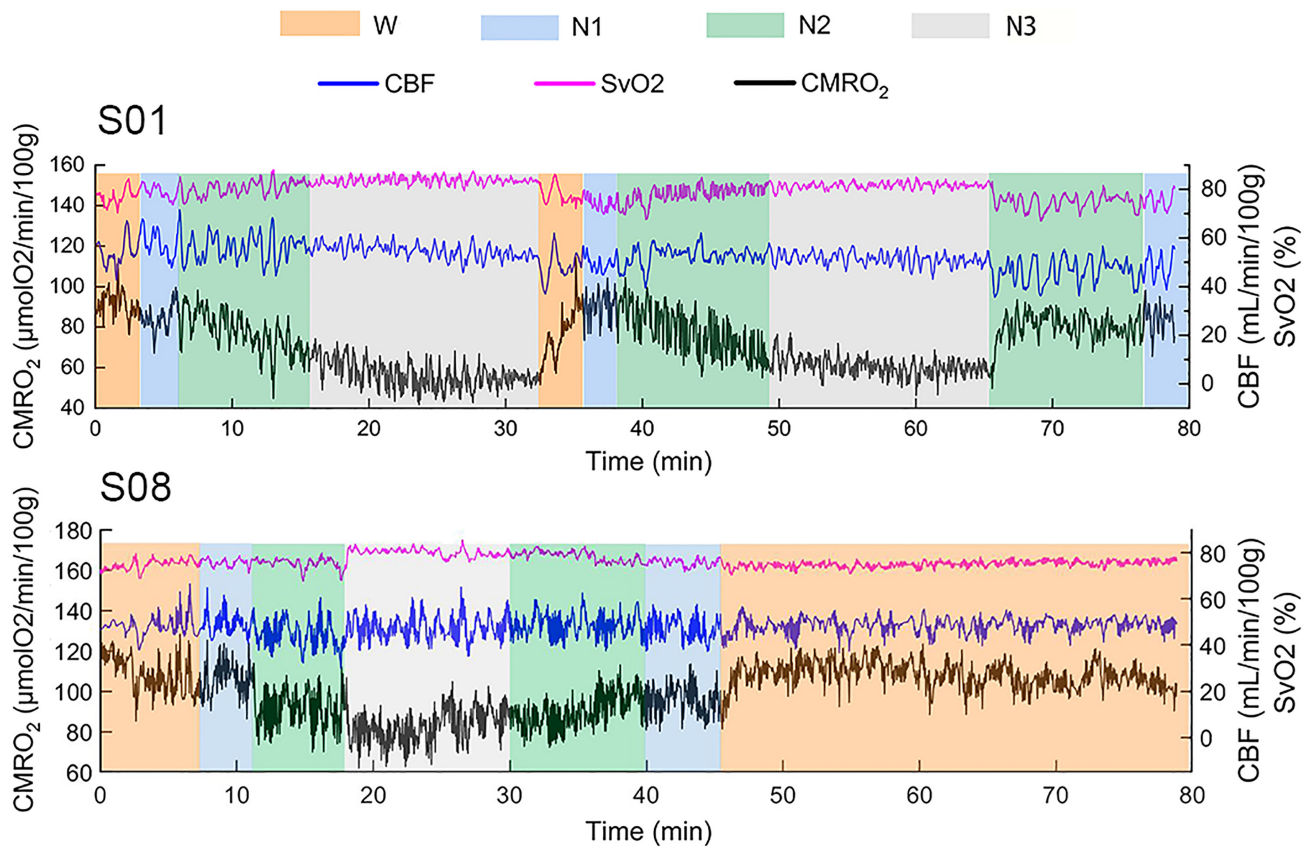
Twenty-one subjects were enrolled in this study. However, two of these were unanalyzable due to excessive head motion, thus 19 subjects are included in the analysis. Among these, 10 achieved N3 sleep including seven young subjects (average age 29 ± 4 years) and three older subjects (average age 68 ± 7 years). The subject demographics and the duration of different sleep stages are given in Table 1. Four individuals were able to achieve more than 20 min of N3 sleep during the 80-min imaging sessions whereas the remaining participants who underwent all sleep stages achieved only 5 min of stage-3 sleep. However, of note is that all 19 subjects yielding evaluable data achieved N1 and 16 achieved both N1 and N2 sleep, while 10 achieved all three sleep stages.

3.2 | EEG-correlated sleep data in subjects who attained all sleep stages

Figure 3 shows CBF, SvO₂, and CMRO₂ time-series for two subjects who achieved N3. Subject S1 (female, 27 years) exhibits a

TABLE 1 Demographics and duration of individual sleep stage during 80 min of scanning.

Participant ID	Age	Gender	Duration of N1 (min)	Duration of N2 (min)	Duration of N3 (min)
s01	27	F	9	32	33
s02	27	F	17	16	21
s03	26	F	13	24	36
s04	31	M	22	38	8
s05	38	M	5	9	5
s06	23	M	16	26	27
s07	28	M	10	13	5
s08	63	M	10	17	12
s09	70	F	8	11	5
s10	62	F	11	48	18
s11	32	F	12	0	0
s12	63	F	12	9	0
s13	29	M	12	16	0
s14	33	F	10	13	0
s15	24	F	5	0	0
s16	30	F	4	0	0
s17	74	F	5	14	0
s18	23	F	7	4	0
s19	64	M	5	5	0

FIGURE 3 Physiological parameters (SvO₂, CBF, CMRO₂) during wakefulness and non-REM sleep for two of the subjects who achieved N3 sleep: S01 (female, age 27 years) and S8 (male, 63 years). For detail, see text.

typical non-REM sleep pattern. $CMRO_2$ decreases gradually during the first non-REM sleep cycle (from $t=0$ to $t=32$ min). The subject achieved N3 at $t=15$ min, and $CMRO_2$ reached a nadir at $t=25$ min. Subsequently, the subject awakens from N3 at $t=32$ min, coincident with a sharp increase in $CMRO_2$ and descends into deep sleep again, repeating the earlier pattern. Also notable is the elevation in SvO_2 and decrease in CBF during deeper sleep stages. Subject S8 (male, 63 years) achieved slow-wave sleep at $t=18$ min, with a duration of N3 of about 12 min. Again, notable is the elevation of SvO_2 while in this subject the sleep-related change in CBF is smaller.

Figure 4 displays EEG power spectra pertaining to the observed states in Subject 01 of Figure 3, highlighting the dominant alpha band at 8–12 Hz during the wake state with eyes closed, the emergence of the theta band (4–8 Hz) during N1, and more prominently during N2, with a concomitant drop in alpha power, and finally the dominance of the delta peak during slow-wave sleep N3.

Average CBF, SvO_2 , and $CMRO_2$ for various sleep stages are presented in Table 2 and Figure 5. The changes from wakefulness to N1 sleep encompassing all subjects ($N=19$) are given in

Figure 5a. The data suggest insignificant decrease in CBF and increase in SvO_2 which, however, together resulted in a significant decrease in $CMRO_2$ of 6.5% ($p < .005$). Figure 5b shows the changes in the vascular-metabolic parameters from wakefulness to N1 and N2 comprising all subjects who achieved both N1 and N2 stage ($N=16$). The trends in the changes in CBF and SvO_2 seen between wakefulness and N1 are evident also for N2 but again, were found not to be significant. In contrast, however, the decrements in $CMRO_2$ are highly significant with changes from wakefulness to N1 and N2 of 6.5 and 10.1% ($p < .005$ and $< .0001$). Finally, the sleep-stage induced changes in CBF, SvO_2 , and $CMRO_2$ for subjects who experienced all three sleep stages ($N=10$) are displayed in Figure 5c. The data in this subset of subjects indicate SvO_2 to be significantly elevated relative to wakefulness at N3 relative to wakefulness as well as N1 and N2 reflecting reduced oxygen extraction fraction. Together, the reduction in oxygen demand is evident from the sharp drop in $CMRO_2$. In the awake state, average $CMRO_2$ was 98 ± 7.3 ($\mu\text{mol O}_2 \text{ min}^{-1}/100 \text{ g}$), falling to 94 ± 10.8 (N1), 91 ± 11.4 (N2), and $76 \pm 9.0 \mu\text{mol min}^{-1}/100 \text{ g}$ (N3), with the mean values at each stage differing significantly from those during wakefulness.

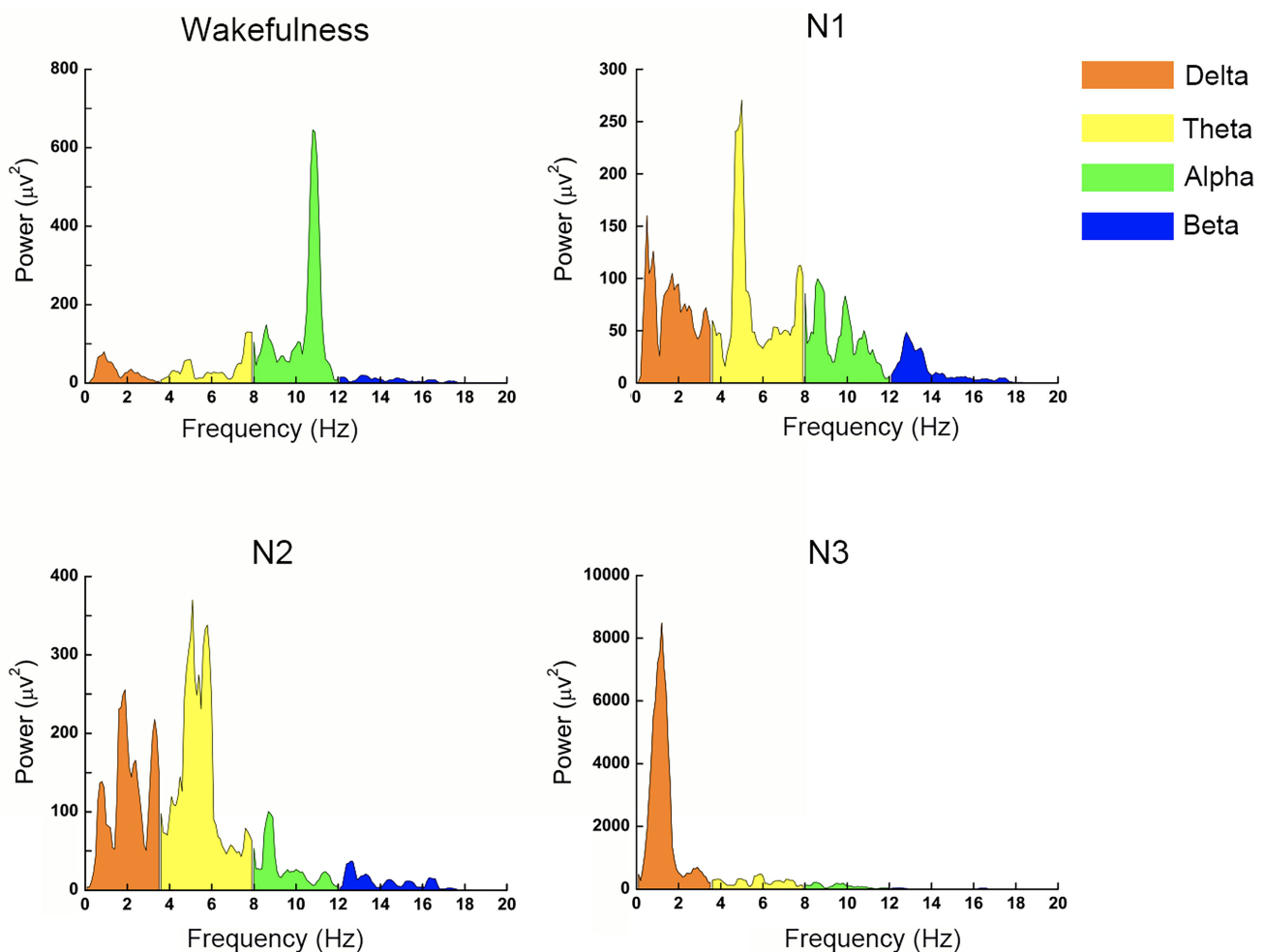


FIGURE 4 EEG power spectra, recorded during the first sleep cycle of Subject S01 (see Figure 3). For detail, see text.

TABLE 2 Average CBF, SvO₂, and CMRO₂ during various sleep stages for subjects who achieved stage-3 sleep.

Participant ID	CBF (mL/min/100g)			SvO ₂ (%)			CMRO ₂ (μmol O ₂ /min/100g)			Change of CMRO ₂ (%)					
	W	N1	N2	N3	W	N1	N2	N3	W	N1	N2	N3	N1 vs W	N2 vs W	N3 vs W
	s01	53.7	48.9	54.0	52.6	77.1	75.4	78.7	82.9	88.7	88.1	80.2	61.0	-7	-9.6
s02	53.6	49.8	50.0	48.2	74.2	75.9	75.4	77.0	90.9	77.1	80.6	70.7	-15.1	-11.3	-22.2
s03	86.9	73.6	77.0	80.8	82.4	78.8	80.4	84.1	111.4	112.5	110.9	90.8	1.0	-4	-18.5
s04	49.3	47.3	45.3	42.4	76.1	75.2	75.7	77.5	93.7	93.9	86.0	73.0	.2	-8.2	-22.1
s05	48.3	43.7	44.0	42.1	79.3	79.1	78.9	81.9	95.1	87.2	87.2	70.1	-8.4	-8.4	-26.3
s06	50.8	51.2	49.5	48.5	81.0	83.5	84.3	85.5	91.5	80.7	73.8	67.2	-11.9	-19.4	-26.7
s07	71.2	69.4	79.9	65.3	83.1	83.1	85.4	84.9	101.1	98.3	98.7	80.2	-2.8	-2.3	-20.6
s08	47.7	46.9	45.5	47.8	75.2	75.9	75.6	79.6	107.6	100.7	98.6	84.2	-6.4	-8.4	-21.8
s09	68.0	68.8	69.4	68.9	82.1	81.8	81.8	84.9	97.2	98.7	98.7	80.2	1.5	1.5	-17.5
s10	54.1	56.1	55.1	53.4	71.6	71.9	72.5	75.9	98.4	102.1	96.4	81.8	3.8	-2.0	-16.9
Average	58.4	55.6	57.0	55.0	78.2	78.1	78.9	81.4	97.5	93.9	91.1	75.9	-3.9	-6.8	-22.4
SD	12.9	10.9	13.5	12.6	3.9	3.8	4.2	3.6	7.4	10.7	11.4	9.0	6.3	6.2	4.5

4 | DISCUSSION

We quantified whole-brain CMRO₂ with concurrent EEG and OxFlow MRI at 2.7s temporal resolution for the duration of a typical sleep cycle. Our results show CMRO₂ to be lower during non-rapid eye movement (non-REM) sleep relative to wakefulness, decreasing progressively toward deeper sleep stages, from a mean of 97.5 ± 7.4 μmol min⁻¹/100g awake to 79.5 ± 9.0 μmol min⁻¹/100g at N3 stage, with the values at wakefulness, N1 and N2 all significantly above N3. The results are a consequence of decreasing oxygen extraction fraction (i.e. increasing SvO₂) and decreasing CBF with depth of sleep stage, commensurate with neuro-vascular-metabolic uncoupling due to gradually reduced neuronal energy demand (Boyle et al., 1994; Madsen & Vorstrup, 1991). Together, these individual vascular-metabolic effects, resulted in a significant reduction in CMRO₂ relative to wakefulness, when the brain is actively engaged in various tasks, as pointed out above. During non-REM sleep, the CMRO₂ drop reflects a reduction in brain activity and concomitant metabolic demand (Boyle et al., 1994; Madsen & Vorstrup, 1991).

There was no evidence of REM sleep in our subjects. In their original work, using tracer-based methods, Madsen et al. found CMRO₂ during REM sleep to be indistinguishable from the wake state (Madsen et al., 1991). Achieving REM sleep in the MRI scanner can be challenging due to the acoustic noise associated with scanning (Wehrle et al., 2007). There are only a limited number of fMRI studies that have successfully obtained REM sleep data, and most of these studies have small sample sizes (Chow et al., 2013; Deuker et al., 2013; Dresler et al., 2011).

We note that the average CMRO₂ during wakefulness in our study (98 μmol O₂ min⁻¹/100g) is lower than in previous findings during the eye-open awake state in the present authors' work (Cao et al., 2018; Caporale et al., 2021; Jain et al., 2010; Rodgers et al., 2013) and elsewhere (Peng et al., 2014; Xu et al., 2009). For instance, Cao et al., reported CMRO₂ of 120.1 ± 19.6 mol O₂/min/100g with rOxFlow at 1.5T in 10 subjects (Cao et al., 2018), Rodgers et al. found 125 ± 11.4 μmol O₂/min/100g using Cartesian OxFlow at 3.0T in 10 subjects (Rodgers et al., 2013), and Caporale et al. obtained 116.9 ± 12 μmol O₂/min/100g with rOxFlow at 3.0T in 12 subjects (Caporale et al., 2021). This discrepancy may be attributed to three factors. First, in the present study, subjects were instructed to close their eyes from the start of the OxFlow time series protocol while being encouraged to sleep. Previous studies have shown that cerebral blood flow (CBF) in the occipital lobe is lower during eye-closed resting state compared to eye-open resting state, while other brain regions did not exhibit significant changes in CBF (Matsutomo et al., 2023; Uludağ et al., 2004). Even though we measure global CMRO₂ and the regional effect is thus diluted, it is likely that overall CMRO₂ is affected in a measurable manner. Second, during the sleep onset latency, that is, during the eyes closed condition, brain activity and thus metabolic demand begin to decrease, leading to a reduction in CMRO₂ ahead of an actual change in sleep stage, relative

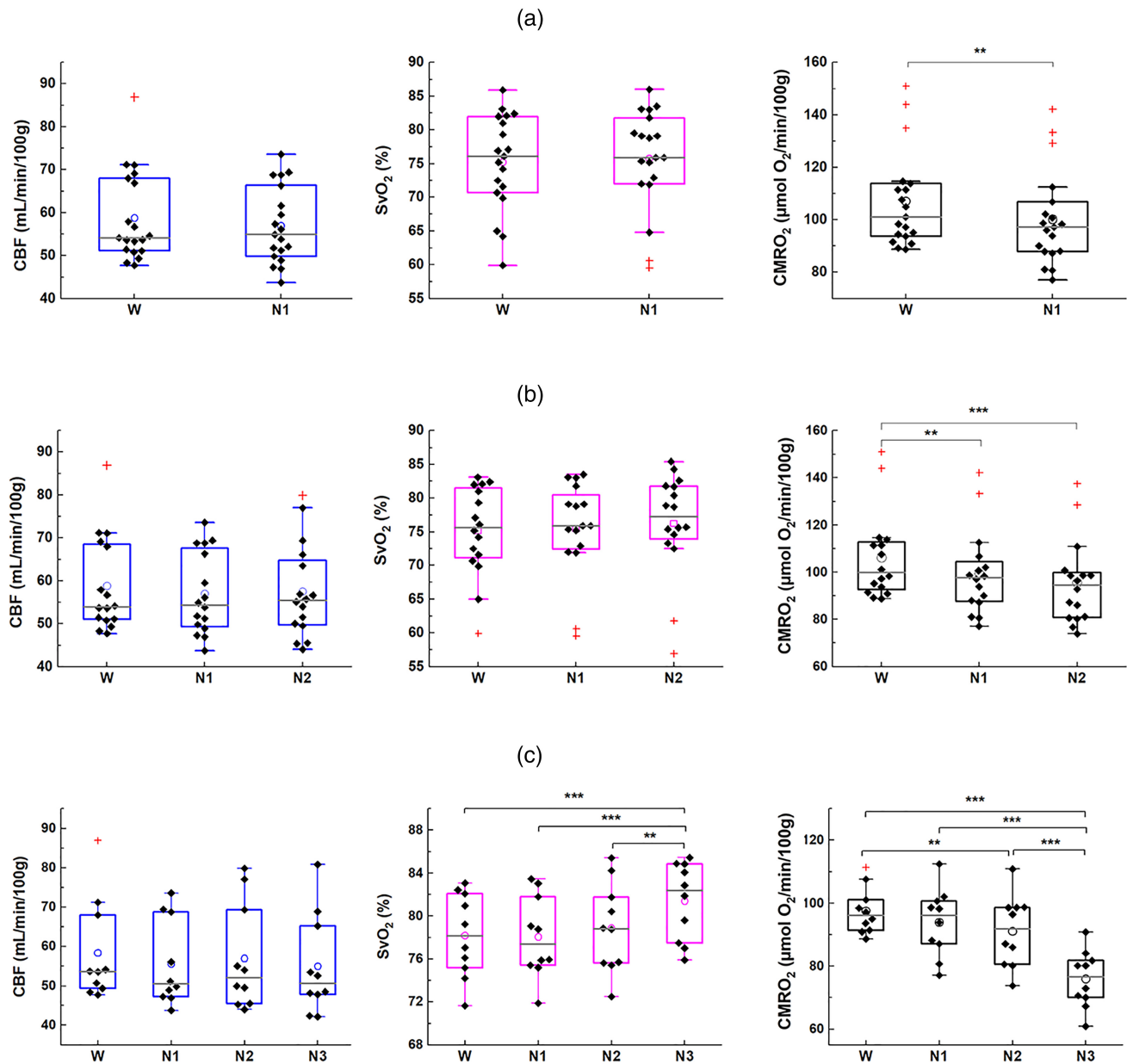


FIGURE 5 Sleep-stage induced changes in vascular-metabolic parameters for: (a) 19 subjects who had only achieved N1 sleep, (b) 16 subjects who had achieved both N1 and N2 sleep, (c) 10 subjects who had gone from wakefulness through all three sleep stages. Boxplots: upper (lower) box edges encompass 25th (75th) percentiles; central gray line represent median; central open circle mean, and whiskers extend to the most extreme data points not considered outliers; red crosses designate outliers (* $p < .01$, ** $p < .005$, *** $p < .0001$).

to their “eyes open” condition. Third, according to the American Academy of Sleep Medicine (AASM) criteria, sleep stages are classified in 30-s epochs, and an epoch with more than 50% (i.e., 15s) of alpha wave activity is scored as wakefulness. As a result, epochs classified as wakefulness may include short phases of non-REM sleep.

The present work has limitations. OxFlow MRI, with both CBF and SvO₂ measurement conducted at the SSS, is currently the highest temporal-resolution method for absolute CMRO₂ quantification, typically allowing for a frame rate of 2–3 s (Cao et al., 2018; Rodgers et al., 2013). However, such time resolution, of course, is achieved at the expense of much reduced spatial resolution

(here, whole-brain vs regional or voxel-wise mapping). Emerging voxel-wise brain oximetric approaches, on the other hand, take anywhere from 10–20 min data collection time and would therefore not be suited for dynamic studies (see, for instance, [Cho et al., 2018; Lee & Wehrli, 2022]).

Among other limitations is that 50% of the subjects in this study did not succeed in achieving deep sleep during the in-scanner sleep study. Unfortunately, MRI scanners do not provide an environment conducive of promoting sleep, given the space constraints and acoustic noise exposure. Active sleep deprivation and sleep-inducing drugs would undoubtedly enhance the success rate (though the latter would likely alter cerebral oxygen metabolism). A recent study

found that with very rigorous screening and enrollment criteria, along with new active acoustic noise control technology, the yield of successful sleep studies can significantly be improved (Moehlman et al., 2019).

Nevertheless, the observed associations between brain energy demand and sleep stage add to our knowledge of sleep physiology while providing a noninvasive method suited for studying the neurometabolic consequences of sleep disorders.

5 | CONCLUSIONS

High temporal resolution OxFLOW MRI with concurrent EEG is able to quantify cerebral oxygen metabolism during wakefulness and sleep. Results indicate brain oxygen consumption to be closely associated with depth of sleep, with deeper non-REM sleep stages exhibiting progressively lower CMRO₂ levels.

DECLARATION OF TRANSPARENCY

The authors, reviewers and editors affirm that in accordance to the policies set by the *Journal of Neuroscience Research*, this manuscript presents an accurate and transparent account of the study being reported and that all critical details describing the methods and results are present.

AUTHOR CONTRIBUTIONS

Visualization, writing/original draft preparation, writing/review & editing, investigation, validation, formal analysis, data curation: Jing Xu; *Investigation, data curation, formal analysis:* Andrew Wiemken; *Conceptualization, investigation, methodology:* Michael C. Langham; *Conceptualization, methodology:* Hengyi Rao; *Investigation:* Marianne Nabbout; *Visualization, writing/review & editing:* Alessandra S. Caporale; *Conceptualization, methodology:* Richard J. Schwab; *Conceptualization, methodology:* John A. Detre; *Lead: conceptualization, funding acquisition, methodology, supervision, writing/review & editing:* Felix W. Wehrli.

ACKNOWLEDGMENTS

The authors disclose receipt of the following financial support for the research, authorship, and/or publication of this article: Research reported in this publication was supported by National Institutes of Health (NIH) grants R21 AG065816 and P41 EB029460 and, in part, by the National Center for Advancing Translational Sciences of the NIH under Award Number UL1TR001878.

CONFLICT OF INTEREST STATEMENT

All authors declare that they have no conflicts of interest.

PEER REVIEW

The peer review history for this article is available at <https://www.webofscience.com/api/gateway/wos/peer-review/10.1002/jnr.25313>.

DATA AVAILABILITY STATEMENT

The data that support the findings of this study are available from the corresponding author upon reasonable request.

ORCID

Alessandra S. Caporale  <https://orcid.org/0000-0002-2182-8312>

Felix W. Wehrli  <https://orcid.org/0000-0003-3430-1840>

REFERENCES

- Allen, P. J., Josephs, O., & Turner, R. (2000). A method for removing imaging artifact from continuous EEG recorded during functional MRI. *NeuroImage*, 12(2), 230–239. <https://doi.org/10.1006/nimg.2000.0599>
- Al-Salman, W., Li, Y., Oudah, A. Y., & Almagid, S. (2023). Sleep stage classification in EEG signals using the clustering approach based probability distribution features coupled with classification algorithms. *Neuroscience Research*, 188, 51–67. <https://doi.org/10.1016/j.neures.2022.09.009>
- Boyle, P. J., Scott, J. C., Krentz, A. J., Nagy, R. J., Comstock, E., & Hoffman, C. (1994). Diminished brain glucose metabolism is a significant determinant for falling rates of systemic glucose utilization during sleep in normal humans. *The Journal of Clinical Investigation*, 93(2), 529–535. <https://doi.org/10.1172/JCI117003>
- Buysse, D. J., Reynolds, C. F., 3rd, Monk, T. H., Berman, S. R., & Kupfer, D. J. (1989). The Pittsburgh sleep quality index: A new instrument for psychiatric practice and research. *Psychiatry Research*, 28(2), 193–213. [https://doi.org/10.1016/0165-1781\(89\)90047-4](https://doi.org/10.1016/0165-1781(89)90047-4)
- Cao, W., Chang, Y. V., Englund, E. K., Song, H. K., Barhoum, S., Rodgers, Z. B., Langham, M. C., & Wehrli, F. W. (2018). High-speed whole-brain oximetry by golden-angle radial MRI. *Magnetic Resonance in Medicine*, 79(1), 217–223. <https://doi.org/10.1002/mrm.26666>
- Caporale, A. S., Barclay, A. M., Xu, J., Rao, H., Lee, H., Langham, M. C., Detre, J. A., & Wehrli, F. W. (2023). Superior sagittal sinus flow as a proxy for tracking global cerebral blood flow dynamics during wakefulness and sleep. *Journal of Cerebral Blood Flow and Metabolism*, 43(8), 1340–1350. <https://doi.org/10.1177/0271678x231164423>
- Caporale, A. S., Lee, H., Lei, H., Rao, H., Langham, M. C., Detre, J. A., Wu, P.-H., & Wehrli, F. W. (2021). Cerebral metabolic rate of oxygen during transition from wakefulness to sleep measured with high temporal resolution OxFLOW MRI with concurrent EEG. *Journal of Cerebral Blood Flow & Metabolism*, 41(4), 780–792.
- Cho, J., Kee, Y., Spincemille, P., Nguyen, T. D., Zhang, J., Gupta, A., Zhang, S., & Wang, Y. (2018). Cerebral metabolic rate of oxygen (CMRO₂) mapping by combining quantitative susceptibility mapping (QSM) and quantitative blood oxygenation level-dependent imaging (qBOLD). *Magnetic Resonance in Medicine*, 80(4), 1595–1604. <https://doi.org/10.1002/mrm.27135>
- Chow, H. M., Horovitz, S. G., Carr, W. S., Picchioni, D., Coddington, N., Fukunaga, M., Xu, Y., Balkin, T. J., Duyn, J. H., & Braun, A. R. (2013). Rhythmic alternating patterns of brain activity distinguish rapid eye movement sleep from other states of consciousness. *Proceedings of the National Academy of Sciences of the United States of America*, 110(25), 10300–10305.
- D'Almeida, V., Lobo, L. L., Hipolide, D. C., de Oliveira, A. C., Nobrega, J. N., & Tufik, S. (1998). Sleep deprivation induces brain region-specific decreases in glutathione levels. *Neuroreport*, 9(12), 2853–2856.
- Deuker, L., Olligs, J., Fell, J., Kranz, T. A., Mormann, F., Montag, C., Reuter, M., Elger, C. E., & Axmacher, N. (2013). Memory consolidation by replay of stimulus-specific neural activity. *Journal of Neuroscience*, 33(49), 19373–19383.
- Dresler, M., Koch, S. P., Wehrle, R., Spoormaker, V. I., Holsboer, F., Steiger, A., Sämann, P. G., Obrig, H., & Czisch, M. (2011). Dreamed

- movement elicits activation in the sensorimotor cortex. *Current Biology*, 21(21), 1833–1837.
- Fernandez-Seara, M. A., Rodgers, Z. B., Englund, E. K., & Wehrli, F. W. (2016). Calibrated bold fMRI with an optimized ASL-BOLD dual-acquisition sequence. *NeuroImage*, 142, 474–482. <https://doi.org/10.1016/j.neuroimage.2016.08.007>
- Fernández-Seara, M. A., Techawiboonwong, A., Detre, J. A., & Wehrli, F. W. (2006). MR susceptometry for measuring global brain oxygen extraction. *Magnetic Resonance in Medicine*, 55, 967–973. <https://doi.org/10.1002/mrm.20892>
- Fukuyama, H., Ogawa, M., Yamauchi, H., Yamaguchi, S., Kimura, J., Yonekura, Y., & Konishi, J. (1994). Altered cerebral energy metabolism in Alzheimer's disease: A PET study. *Journal of Nuclear Medicine*, 35(1), 1–6.
- Girouard, H., & Iadecola, C. (2006). Neurovascular coupling in the normal brain and in hypertension, stroke, and Alzheimer disease. *Journal of Applied Physiology*, 100, 328–335.
- Gopalakrishnan, A., Ji, L. L., & Cirelli, C. (2004). Sleep deprivation and cellular responses to oxidative stress. *Sleep*, 27(1), 27–35.
- Iber, C., Ancoli-Israel, S., Chesson, A. L., & Quan, S. (2007). *The AASM manual for the scoring of sleep and associated events: Rules, terminology and technical specifications*. American Academy of Sleep Medicine.
- Ishii, K., Kitagaki, H., Kono, M., & Mori, E. (1996). Decreased medial temporal oxygen metabolism in Alzheimer's disease shown by PET. *Journal of Nuclear Medicine*, 37(7), 1159–1165.
- Jain, V., Langham, M. C., & Wehrli, F. W. (2010). MRI estimation of global brain oxygen consumption rate. *Journal of Cerebral Blood Flow & Metabolism*, 30(9), 1598–1607. <https://doi.org/10.1038/jcbfm.2010.49>
- Kastrup, A., Kruger, G., Neumann-Haefelin, T., Glover, G. H., & Moseley, M. E. (2002). Changes of cerebral blood flow, oxygenation, and oxidative metabolism during graded motor activation. *NeuroImage*, 15(1), 74–82. <https://doi.org/10.1006/nimg.2001.0916>
- Langham, M. C., Magland, J. F., Floyd, T. F., & Wehrli, F. W. (2009). Retrospective correction for induced magnetic field inhomogeneity in measurements of large-vessel hemoglobin oxygen saturation by MR susceptometry. *Magnetic Resonance in Medicine*, 61, 626–633. <https://doi.org/10.1002/mrm.21499>
- Lee, H., & Wehrli, F. W. (2022). Whole-brain 3D mapping of oxygen metabolism using constrained quantitative BOLD. *NeuroImage*, 250, 118952. <https://doi.org/10.1016/j.neuroimage.2022.118952>
- Madsen, P. L., Schmidt, J. F., Wildschjødts, G., Friberg, L., Holm, S., Vorstrup, S., & Lassen, N. A. (1991). Cerebral O₂ metabolism and cerebral blood flow in humans during deep and rapid-eye-movement sleep. *Journal of Applied Physiology*, 70, 2597–2601.
- Madsen, P. L., & Vorstrup, S. (1991). Cerebral blood flow and metabolism during sleep. *Cerebrovascular and Brain Metabolism Reviews*, 3(4), 281–296.
- Magistretti, P. J., & Allaman, I. (2015). A cellular perspective on brain energy metabolism and functional imaging. *Neuron*, 86(4), 883–901. <https://doi.org/10.1016/j.neuron.2015.03.035>
- Matsutomo, N., Fukami, M., Kobayashi, K., Endo, Y., Kuhara, S., & Yamamoto, T. (2023). Effects of eyes-closed resting and eyes-open conditions on cerebral blood flow measurement using arterial spin labeling magnetic resonance imaging. *Neurology and Clinical Neuroscience*, 11(1), 10–16. <https://doi.org/10.1111/ncn3.12674>
- Mintun, M. A., Raichle, M. E., Martin, W. R., & Herscovitch, P. (1984). Brain oxygen utilization measured with O-15 radiotracers and positron emission tomography. *Journal of Nuclear Medicine*, 25(2), 177–187.
- Moehلمان, T. M., de Zwart, J. A., Chappel-Farley, M. G., Liu, X., McClain, I. B., Chang, C., Mandelkow, H., Özbay, P. S., Johnson, N. L., Bieber, R. E., Fernandez, K. A., King, K. A., Zalewski, C. K., Brewer, C. C., van Gelderen, P., Duyn, J. H., & Picchioni, D. (2019). All-night functional magnetic resonance imaging sleep studies. *Journal of Neuroscience Methods*, 316, 83–98. <https://doi.org/10.1016/j.jneumeth.2018.09.019>
- Oshima, T., Karasawa, F., & Satoh, T. (2002). Effects of propofol on cerebral blood flow and the metabolic rate of oxygen in humans. *Acta Anaesthesiologica Scandinavica*, 46(7), 831–835. <https://doi.org/10.1034/j.1399-6576.2002.460713.x>
- Peng, S. L., Dumas, J. A., Park, D. C., Liu, P., Filbey, F. M., McAdams, C. J., Pinkham, A. E., Adinoff, B., Zhang, R., & Lu, H. (2014). Age-related increase of resting metabolic rate in the human brain. *NeuroImage*, 98, 176–183. <https://doi.org/10.1016/j.neuroimage.2014.04.078>
- Rodgers, Z. B., Jain, V., Englund, E. K., Langham, M. C., & Wehrli, F. W. (2013). High temporal resolution MRI quantification of global cerebral metabolic rate of oxygen consumption in response to apneic challenge. *Journal of Cerebral Blood Flow & Metabolism*, 33(10), 1514–1522. <https://doi.org/10.1038/jcbfm.2013.110>
- Uludağ, K., Dubowitz, D. J., Yoder, E. J., Restom, K., Liu, T. T., & Buxton, R. B. (2004). Coupling of cerebral blood flow and oxygen consumption during physiological activation and deactivation measured with fMRI. *NeuroImage*, 23(1), 148–155. <https://doi.org/10.1016/j.neuroimage.2004.05.013>
- Wehrle, R., Kaufmann, C., Wetter, T. C., Holsboer, F., Auer, D. P., Pollmächer, T., & Czisch, M. (2007). Functional microstates within human REM sleep: First evidence from fMRI of a thalamocortical network specific for phasic REM periods. *European Journal of Neuroscience*, 25(3), 863–871.
- Wehrli, F. W., Fan, A. P., Rodgers, Z. B., Englund, E. K., & Langham, M. C. (2017). Susceptibility-based time-resolved whole-organ and regional tissue oximetry. *NMR in Biomedicine*, 30(4), e3495.
- Xu, F., Ge, Y., & Lu, H. (2009). Noninvasive quantification of whole-brain cerebral metabolic rate of oxygen (CMRO₂) by MRI. *Magnetic Resonance in Medicine*, 62(1), 141–148. <https://doi.org/10.1002/mrm.21994>

SUPPORTING INFORMATION

Additional supporting information can be found online in the Supporting Information section at the end of this article.

Data S1: Transparent Science Questionnaire for Authors.

How to cite this article: Xu, J., Wiemken, A., Langham, M. C., Rao, H., Nabbout, M., Caporale, A. S., Schwab, R. J., Detre, J. A., & Wehrli, F. W. (2024). Sleep-stage-dependent alterations in cerebral oxygen metabolism quantified by magnetic resonance. *Journal of Neuroscience Research*, 102, e25313. <https://doi.org/10.1002/jnr.25313>